

Microfluidic Purification and Preconcentration of mRNA by Flow-Through Polymeric Monolith

Brent C. Satterfield,^{†,‡} Seth Stern,[†] Michael R. Caplan,[‡] Kyle W. Hukari,[†] and Jay A. A. West*[†]

Arcxis Biotechnologies, Pleasanton, California 94566, and Harrington Department of Bioengineering, Arizona State University, Tempe, Arizona 85287-9709

Efficient and rapid isolation of mRNA is important in the field of genomics as well as in the clinical and pharmaceutical arena. We have developed UV-initiated methacrylate-based porous polymer monoliths (PPM) for microfluidic trapping and concentration of eukaryotic mRNA. PPM are cast-to-shape and are tunable for functionalization using a variety of amine-terminated molecules. Efficient isolation of eukaryotic mRNA from total RNA was first mathematically modeled and then achieved using PPM in capillaries. Purification protocols using oligo dT's, locked nucleic acid substituted dT's, and tetramethylammonium chloride salts were characterized. mRNA yield and purity were compared with mRNA isolated by commercial kits with statistically equivalent yields and purities (determined by qPCR ratio of 18s rRNA and Gusb mRNA markers). Even after extracting 16 μg of mRNA from 315 μg of total RNA, the 0.4- μL volume monolith showed no signs of saturation. Elution volumes were below 20 μL with concentrations up to 1 $\mu\text{g}/\mu\text{L}$. In addition, the polymeric material exhibited exceptional stability in a range of conditions (pH, temperature, dryness) and was stable for a period of months. All of these characteristics make porous polymer monoliths good candidates for potential microfluidic sample preconcentrators and purifiers.

The aims of microfluidics include faster, less expensive, and more sensitive portable technologies.^{1,2} However, real world samples present a major challenge in device functionality. As a result, the benefits of microfluidic analysis apply only to highly purified and highly concentrated samples.^{3,4} Thus, there is a need for efficient and portable sample preparation technologies.

Many end point analyses require some form of sample preconcentration.⁵ mRNA as a polynucleotide analyte has particular utility. It represents the active counterpart to DNA, or the primary analogue of DNA that is actively engaged in phenotypic

expression in an organism. It is typically extracted from eukaryotic cells via its polyadenosine tail (poly-A); mRNA extraction is based on the interactions between a sequence of polythymine deoxyribonucleotides (oligo dT's) and the poly-A tail of mRNA. The use of functionalized cellulose to selectively extract polynucleotides was developed early in the 1960s.^{6–9} The integration of oligo dT's, specifically for the purpose of mRNA purification, with cellulose columns, cellulose powders, polymeric beads, and magnetic beads was an innovation that followed.^{10,11}

Examples of mRNA preconcentration and purification in microfluidics are rare. Jiang and Harrison previously reported the ability to integrate mRNA isolation using magnetic beads on a microfluidic device.¹² In these studies, the mRNA was first isolated on magnetic beads in a microfluidic channel. Then, the beads were removed, and the residual nonhybridized material was washed away. This reported device required only 20 min of flow time, trapped up to 60 ng of mRNA, and offered 26% efficiency compared to off-chip methods.¹²

Recently, functionalized photopolymerizable monoliths have been used as an alternative to traditional sample preparation methods for chemicals,¹³ polypeptides,^{14,15} and polynucleotides,¹⁶ most of these being used in conjunction with capillary electrochromatography or HPLC. These materials have been reviewed extensively in a work compiled and edited by Svec et al.¹⁷ These monoliths provide high surface area for adsorption of the analyte of interest¹⁸ and are easily and cost-effectively created inside of microfluidic channels through UV-light exposure. Variable pore

* To whom correspondence should be addressed. E-mail: jwest@arcxis.com. Phone: (925) 461-1300.

[†] Arcxis Biotechnologies.

[‡] Arizona State University.

- (1) Selvaganapathy, P. R.; Carlen, E. T.; Mastrangelo, C. H. *Proc. IEEE* **2003**, *91*, 954–975.
- (2) Saito, Y.; Kawazoe, M.; Imaizumi, M.; Morishima, Y.; Nakao, Y.; Hatano, K.; Hayashida, M.; Jinno, K. *Anal. Sci.* **2002**, *18*, 7–17.
- (3) Verpoorte, E. *Electrophoresis* **2002**, *23*, 677–712.
- (4) de Mello, A. J.; Beard, N. *Lab Chip* **2003**, *3*, 11N–19N.
- (5) Lichtenberg, J.; de Rooij, N. F.; Verpoorte, E. *Talanta* **2002**, *56*, 233–266.

- (6) Bautz, E. K.; Hall, B. D. *Proc. Natl. Acad. Sci. U.S.A.* **1962**, *48*, 400–408.
- (7) Gilham, P. T. *J. Am. Chem. Soc.* **1962**, *84*, 1311–1312.
- (8) Gilham, P. T. *J. Am. Chem. Soc.* **1964**, *86*, 4982–4985.
- (9) Gilham, P. T. *Biochemistry* **1968**, *7*, 2809–2813.
- (10) Aviv, H.; Leder, P. *Proc. Natl. Acad. Sci. U.S.A.* **1972**, *69*, 1408–1412.
- (11) Hornes, E.; Korsnes, L. *Genet. Anal. Technol. Appl.* **1990**, *7*, 145–150.
- (12) Jiang, G.; Harrison, D. J. *Analyst* **2000**, *125*, 2176–2179.
- (13) Yu, C.; Davey, M. H.; Svec, F.; Frechet, J. M. *Anal. Chem.* **2001**, *73*, 5088–5096.
- (14) Shediach, R.; Ngola, S. M.; Throckmorton, D. J.; Anex, D. S.; Shepodd, T. J.; Singh, A. K. *J. Chromatogr., A* **2001**, *925*, 251–263.
- (15) Throckmorton, D. J.; Shepodd, T. J.; Singh, A. K. *Anal. Chem.* **2002**, *74*, 784–789.
- (16) West, J. A. A.; Hukari, K. W.; Hux, G.; Shepodd, T. J. *Proceedings of the Society of Photo-Optical Instrumentation Engineers (spie) Conference on Lab-on-a-Chip: Platforms, Devices, and Applications Conference on Lab-on-a-Chip: Platforms, Devices, and Applications*; October 26–28, 2004; Philadelphia, PA, **2004**, 5591, 167–173.
- (17) *Monolithic Materials: Preparation, Properties, and Applications*; Elsevier: Amsterdam, 2003.
- (18) Yu, C.; Xu, M. C.; Svec, F.; Frechet, J. M. J. *J. Polym. Sci., Part A: Polym. Chem.* **2002**, *40*, 755–769.

size and porosity can be achieved based on concentration and type of porogenic solvent.¹³ PPMs also exhibit good surface adhesion and form stable bonds with channel walls.¹⁹

In this paper, we report an mRNA sample preconcentration method that allows for facile incorporation into a microfluidic detection unit and, despite its submicroliter volume, is able to trap and purify mRNA in an equivalent fashion as nonmicrofluidic, commercial kits. Using a photoinitiated monolith that is polymerized and functionalized in situ, we were able to take advantage of the large surface area and controllable pore size inherent to monoliths. High efficiencies, purification ability, and fast hybridization times show that the oligonucleotide functionalized porous polymer monoliths will be an ideal method for mRNA sample preparation in microfluidic devices.

EXPERIMENTAL SECTION

Reagents and Supplies. The following chemicals were used without further purification at various steps of experimentation. Glycidyl methacrylate (GMA), ethylene glycol dimethacrylate (EGDMA), ethyl acetate, sodium dodecyl sulfate (SDS), NaCl, 2-propanol, propylamine, tetramethylammonium chloride (TMAC), and methanol were purchased from Aldrich Chemical Co. DEPC water, sodium phosphate buffers, Tris-HCl buffers, poly-A purist mRNA purification kit, rat liver total RNA, and rat liver mRNA were purchased from Ambion. Ambion mRNA and kits were chosen because they have consistently provided the highest quality commercial mRNA in our hands. Z-6030 silane was obtained from Dow Corning (Midland, MI). Labeled and unlabeled oligo-dT's were synthesized by Biosearch Technologies (Novato, CA). The 20-mer oligo dT's substituted with 50% locked nucleic acid (LNA) analogues and 100% LNA were synthesized by Sigma-Proligo. Microfluidic components were purchased from LabSmith (Livermore, CA) and capillaries from PolyMicro Technologies (Phoenix, AZ). Primers, probes, and other PCR reagents were purchased from Applied Biosystems (Foster City, CA).

Porous Polymer Monoliths. Trapping of target oligonucleotides was accomplished using a UV-cured porous polymer monolith (PPM) that was fabricated in a fused-silica capillary. Briefly, capillaries were pretreated with a mixture of 0.4% v/v z-6030 silane in 2-propanol. The solution was used to fill the capillaries, which were incubated for 15 min at 90 °C. The monomer mixture contained 12.5% v/v 10 mM NaH₂PO₄, pH 7.2, 12.5% ethyl acetate, 40% methanol, 10.5% GMA, and 24.5% EGDMA, also containing 2.5 mg of Irgacure (Ciba Specialty Chemicals, McIntosh, AL). The solution was vortexed until the initiator was solubilized. The capillaries were then filled and photopolymerized at 365 nm using a UV cross-linking oven (Spectronics Corp., Westbury, NY) for 10 min.

Functionalizing PPM. After PPM were formed in the capillary, the material was flushed with 100 μL of DEPC water. We then either functionalized the PPM with primary amine-terminated fluorescent dye molecules, performed in pure acetonitrile, or functionalized the polymers with the oligonucleotide complete with a 5'-NH₃-C6 linked oligo dT (30-mer) with or without a 6-carboxy-fluorescein covalently linked to the oligonucleotide near the 5' terminus. To perform functionalization, oligo dT (500 μM) was

dissolved in a buffer containing 10 mM phosphate buffer, 500 mM NaCl, 0.05–0.1% SDS. The oligonucleotides were then denatured before introducing them to the native PPM. The covalent attachment of oligonucleotides was optimized by performing a series of binding experiments with incubation temperatures of 60, 90, and 120 °C for incubation times of 30, 60, and 120 min. The attachment of the oligo dT was confirmed by imaging the fluorescently derivatized column. Each optimization experiment was repeated three times. Experiments were compared by *t*-test of average fluorescence over the length of the polymer. Although the 120 °C run appeared to work well, the optimal 90 °C incubation for 60 min was used for the remainder of the experiments.

Flow Rate Optimization. Capillaries were functionalized with unlabeled oligo dT's and were blocked with 100 μL of 10 mM Tris-HCl buffer with 180 mM NaCl and 0.1% SDS at 120 °C for 30 s. The 30-μL aliquot of Ambion rat liver mRNA (5 ng/μL) in 10 mM Tris-HCl buffer with 180 mM NaCl and 0.1% SDS was loaded onto each capillary at rates controlled by a syringe pump, which were varied between 2.4 and 76.8 μL/min. During the procedure, the capillary was clamped onto two thermoelectric coolers aligned in succession, allowing both a denaturing and a hybridization zone. The denaturing zone was 3 cm and was maintained at 90 °C, while the hybridization zone was 1 cm and was maintained at 45 °C during loading. The wash step was performed with 30 μL of 10 mM Tris-HCl buffer with 180 mM NaCl at 45 °C at a rate equivalent to the loading rate. Elution was performed in 5–20 μL of DEPC water at 90 °C. Spectrophotometric measurements of all samples before and after purification were made on a NanoDrop 1000 (NanoDrop, Wilmington, DE). Three replicates of each data point were run, and run order was randomized. The efficiency of the extraction was plotted versus contact time with the monolith (monolith length/average fluid velocity). A model describing the initial extraction efficiency (C/T_0 , where C is the concentration of complex formed between oligo dT and mRNA and T_0 is the initial mRNA concentration) as a function of the initial oligo dT concentration (P_0), forward rate constant (k_f), equilibrium constant (K_{eq}), and contact time (t_c) was plotted with the data (assumes $P_0 \gg T_0$):

$$\frac{C}{T_0} = \frac{1}{1 + \frac{1}{P_0 K_{eq}}} f (1 - e^{-k_f P_0 t_c})$$

The contact time was calculated for each flow rate using an 8-mm monolith. Sekar et al. fit rate constants for 24-mer oligonucleotide hybridizations (oligos with no known secondary structures) and obtained values between 1.2×10^4 and $1.2 \times 10^5 \text{ M}^{-1} \text{ s}^{-1}$.²⁰ Since we used 40-mer dT's, we selected the higher value of $1.2 \times 10^5 \text{ M}^{-1} \text{ s}^{-1}$ for our calculations. K_{eq} was calculated from mFold thermodynamic parameter estimates (<http://www.bioinfo.rpi.edu/applications/mfold/>). P_0 was best fit (11 μM) by minimizing the sum of square errors. Since poly-A enriched RNA is not 100% mRNA, a maximum binding constant, f , was added to the equation and was set equal to the average efficiency of the 2.4 and 4.8 μL/min runs.

Bioanalyzer Analysis of mRNA Integrity. Using an Agilent 2100 bioanalyzer with a Pico total RNA chip/protocol, 5 ng of

(19) Ngola, S. M.; Fintschenko, Y.; Choi, W. Y.; Shepodd, T. J. *Anal. Chem.* **2001**, *73*, 849–856.

(20) Sekar, M. M.; Bloch, W.; St, John, P. M. *Nucleic Acids Res.* **2005**, *33*, 366–375.

Ambion rat liver total RNA, Ambion rat liver mRNA and monolith extracted mRNA from the 2.4 $\mu\text{L}/\text{min}$ run in Flow Rate Optimization were analyzed side by side. The data are presented in gel format.

mRNA Purification. Five different capillaries were functionalized with unlabeled oligo dT's and were first blocked with 100 μL of 10 mM Tris-HCl buffer in 180 mM NaCl and 0.1% SDS at 120 $^{\circ}\text{C}$ for 30 s. The 1–315 μg of rat liver total RNA (0.2–1.0 $\mu\text{g}/\mu\text{L}$) with 10 mM Tris-HCl buffer with 180 mM NaCl and 0.1% SDS was loaded onto each capillary at rates controlled by a syringe pump of 5 $\mu\text{L}/\text{min}$. The capillary was clamped onto two thermoelectric coolers as described in Flow Rate Optimization. The wash step was performed with 30 μL of 10 mM Tris-HCl buffer with 180 mM NaCl at 45 $^{\circ}\text{C}$ at 5 $\mu\text{L}/\text{min}$. Elution was performed in 5–20 μL of DEPC water at 90 $^{\circ}\text{C}$. mRNA was also purified from rat liver total RNA by following the protocol of the poly-A purist kit. Spectrophotometric measurements of all samples before and after purification were made on a NanoDrop 1000. The average yield of the five capillaries for five different loading volumes was recorded, and their respective concentrations were plotted.

Several other purification methods were used also, each with three capillaries. Mixed LNA-dT, 100% LNA substituted dT, and oligo dT capillaries were functionalized and then blocked with 1% propylamine in 2-propanol at 90 $^{\circ}\text{C}$ for 15 min. Capillaries were flushed with 100 μL of 10 mM Tris-HCl buffer with 180 mM NaCl and 0.1% SDS. mRNA was bound to mixed LNA-dT columns in 10 mM Tris-HCl buffer with 180 mM NaCl and 0.1% SDS at 45 $^{\circ}\text{C}$ and was washed in 50 mM NaCl in 10 mM Tris-HCl buffer at 45 $^{\circ}\text{C}$. mRNA was eluted at 90 $^{\circ}\text{C}$ in dH_2O . mRNA was bound to 100% LNA substituted dT columns with 10 mM Tris-HCl buffer with 180 mM NaCl and 0.1% SDS at 45 $^{\circ}\text{C}$ and was washed in dH_2O at 0 $^{\circ}\text{C}$. mRNA was eluted at 90 $^{\circ}\text{C}$ in dH_2O . mRNA was bound to oligo-dT columns in 10 mM Tris-HCl buffer with 180 mM TMAC and 0.1% SDS at 45 $^{\circ}\text{C}$ and was washed in 10 mM Tris-HCl buffer in 3 M TMAC at room temperature (24 $^{\circ}\text{C}$). A second wash step of 30 μL over 6 min was performed at 90 $^{\circ}\text{C}$ in 10 mM Tris-HCl buffer in 2 M TMAC. After flushing out salt solutions with air, mRNA was eluted at 90 $^{\circ}\text{C}$ in dH_2O .

qPCR Analysis of mRNA Integrity. Where additional comparison of mRNA quality was required, qPCR was performed for two different targets, one target representing the degree of contamination (18s ribosomal RNA) present in the sample and one target representing the mRNA present in the sample (Gusb mRNA). Predesigned primer and probe sets from Applied Biosystems were used in the quantification of 18s rRNA and Gusb mRNA. Briefly, 7.35 μL of DEPC treated water, 10 μL of 2 \times Taqman fast universal master mix, either 1 μL of 20 \times Gusb primer/probe mix with FAM label or 1 μL of 20 \times 18s primer/probe mix with VIC label, 0.4 μL of 20 units/ μL Rnase inhibitor, 0.25 μL of 50 units/ μL MultiScribe, and 1 μL of RNA were used in each well for amplification on an ABI 7500 PCR machine. The protocol included a 30-min reverse transcriptase step at 48 $^{\circ}\text{C}$, a 20-s activation step at 95 $^{\circ}\text{C}$ followed by 40 cycles of 95 $^{\circ}\text{C}$ for 3 s and 60 $^{\circ}\text{C}$ for 30 s. Standard curves for 18s rRNA and Gusb mRNA were created from four dilutions (50, 10, 2, 0.4 ng) of rat liver total RNA. Fold enrichment was calculated by quantifying 18s and Gusb presence on the total RNA standard curves and then finding the ratio of Gusb mRNA to 18s rRNA.

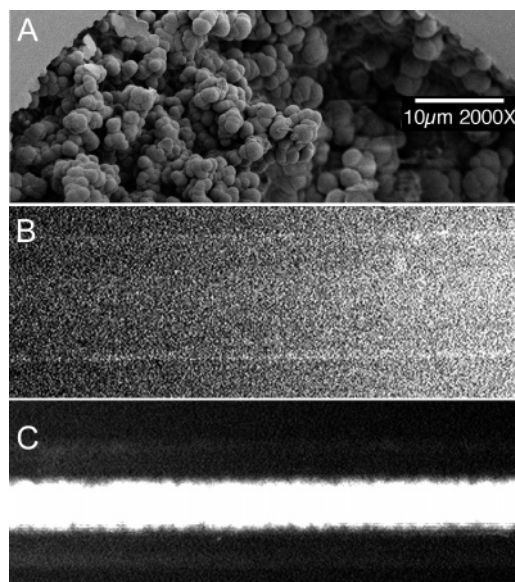


Figure 1. Photopolymerization and postfunctionalization of the monolith material. Reveals SEM image of polymer consistency in the capillary (A) and a high-gain image with no fluorescent marker (B) in contrast to a low-gain image with Oregon Green bound to the PPM (C).

RESULTS AND DISCUSSION

We performed a variety of experiments to determine the optimal scheme for the deposition of glycidyl methacrylate containing PPM in the capillary. These experiments enabled the polymerization of a porous material that readily allows the attachment of various amine-containing compounds (Figure 1). The nodules in these polymer materials appear to be bound to the channel wall (Figure 1A). We found that the polymerized monoliths were rigid and similar to previous studies,^{14,19} mitigating the use of frits to contain the polymer in the capillary channel, and allowed the deposition of the polymer in a discrete location, such as in a microfluidic device. These polymers, as seen in Figure 1A, are homogeneous in nodule size and in porosity, with an approximate pore size of 2–3 μm .

Following the optimization of the monolith material, we optimized the functionalization of the materials. The GMA monomers selected for these studies theoretically allow the attachment of a variety of biological molecules provided the molecule is capable of performing a nucleophilic attack on the intact epoxide ring on the synthesized PPM. Prior to functionalization, there was no discernible fluorescent signal from the PPM. In Figure 1B, the gain was increased to allow the imaging of the capillary, which can be seen upon closer examination. To optimize the conditions for functionalization, we initially made use of a fluorescent dye. Oregon Green Caverdine was employed due to its high fluorescent intensity and the presence of a terminal amine on the dye molecule, enabling direct covalent reactivity with the GMA. In order to functionalize the PPM, the column was filled with Oregon Green Caverdine and allowed to stand overnight at room temperature. After this overnight incubation, the columns were extensively flushed for 3 h to remove unbound dye. Figure 1C is a fluorescent image of a capillary after functionalization with Oregon Green. In contrast to the control image (Figure 1B), an intense fluorescence is present. To ensure the chemistry was stable, these columns were flushed (in the dark) in a variety of

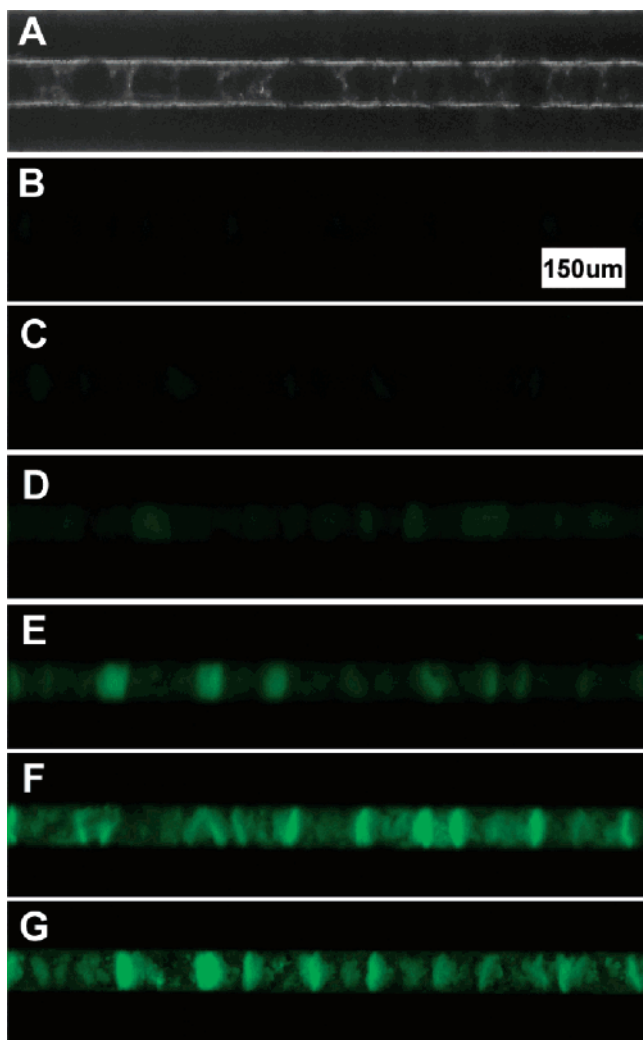


Figure 2. Oligo dT binding optimization. Shows a light microscope image of the capillary with monolith (A) together with oligo binding intensity for different times and temperatures. The images are for 60 °C for 30 (B) and 60 min (C), 90 °C for 30 (D) and 60 min (E), and 120 °C for 30 (F) and 60 min (G).

solvents and pH conditions for as long as one week. Continuous flushing for over a week, with a range of pHs from 3 to 9 did not remove the Oregon Green once bound (data not shown).

Having optimized the attachment of organic compounds to the polymer, we then focused on the functionalization of the polymer monoliths with oligonucleotides (Figure 2). As with the Oregon Green functionalization, the optimization of oligo dT binding was performed under stopped flow conditions in a 75- μm -i.d. capillary (Figure 2A). For incubation conditions of 30 min at 60 °C, as seen in Figure 2B, an extremely faint, if not undetectable, amount of oligo dT is attached to the PPM. When the incubation time was extended to 60 min (Figure 2C), there appeared to be an increase in the fluorescent intensity of the functionalized polymer. Beyond 60 min, the incorporation of the oligo dT was not significantly improved with longer incubation times at this temperature ($p = 0.179$). In contrast, raising the temperature demonstrated the most dramatic effect on functionalization of the PPM. When the temperature of the functionalization reaction was increased to 90 °C from 60 °C, the average fluorescence doubled (Figure 2D). As seen previously, oligo binding increased over time. Increasing

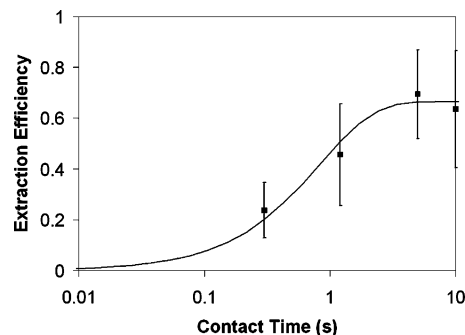


Figure 3. Contact time optimization. Shows the extraction efficiency as a function of the contact time (monolith length/average fluid velocity), which is proportional to the inverse of the flow rate. Data points with 95% confidence intervals are plotted with a theoretical curve.

the incubation time from 30 to 60 min caused the concentration of bound oligos to more than double (Figure 2E). There was no further increase in oligo binding observed at time points greater than 60 min ($p = 0.911$). Maximal binding in the shortest time was found when the temperature of the functionalization was raised to 120 °C. In contrast to previous trials at lower temperatures, incubation times greater than 30 min did not result in increases (compare Figure 2F and G) in fluorescent intensity ($p = 0.776$). The observed plateau in fluorescent intensity was not attributed to signal saturation, since higher fluorescent intensities were observed on the capillaries prior to washing off the excess oligo dT.

Like the dye functionalized PPM, we found that the oligonucleotide functionalized monoliths were exceptionally stable both with various buffers and with solvents. Over 200 μL of pH 9.0 blocking buffer was flushed through the column at 120 °C for more than 1 h with minimally detectable oligo elution or degradation as indicated by fluorescent intensity (data not shown). In addition, we found the functionalized columns were stable over time, as many of these capillaries have been stored over several weeks without noticeable decreases in fluorescent intensity. Taken together, these results indicate that the functionalized polymers should be stable under a broad range of conditions.

One further optimization was required before comparing mRNA extraction methods. Nadin-Davis and Mezl observed the importance of flow rate in mRNA extraction efficiency.²¹ Further, theoretical predictions indicate that efficiency of extraction is exponentially dependent upon contact time with the monolith (a function of the flow rate) in addition to oligo dT concentration and the forward rate constant. Having optimized the oligo dT concentration, and not being able to control the forward rate constant, we needed to optimize the contact time with the monolith, by controlling the flow rates. It was discovered that a contact time of 5 s was sufficient to achieve maximal binding (Figure 3). Using similar flow rates, Jiang and Harrison achieved 26% trapping efficiency with magnetic beads in a microfluidic device.¹² In contrast, with a smaller volume of PPM material, our results indicate a 70% extraction efficiency of mRNA from high-quality commercial poly-A-enriched RNA.

We anticipated maximal extraction efficiencies of mRNA closer to 100%. To explain the discrepancy, we performed microchip

(21) Nadin-Davis, S.; Mezl, V. A. *J. Biochem. Biophys. Methods* **1985**, *11*, 185–189.

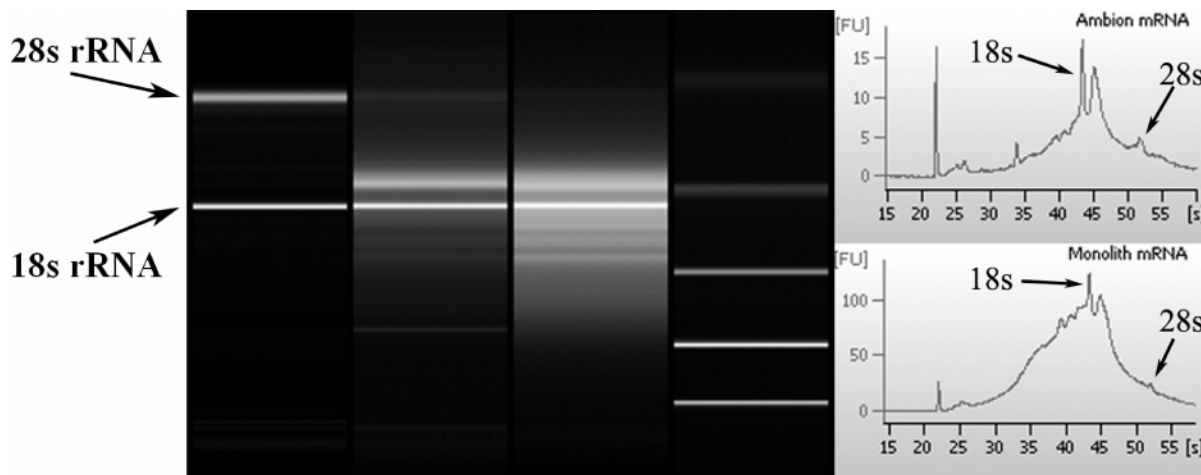


Figure 4. Enrichment of mRNA trapped on monoliths (lane 3) from Ambion mRNA (lane 2) next to total RNA (lane 1) and an RNA ladder (0.2, 0.5, 1.0, 2.0, 4.0 kb, lane 4). Figures on right show electropherograms of lane 2 (top) and lane 3 (bottom).

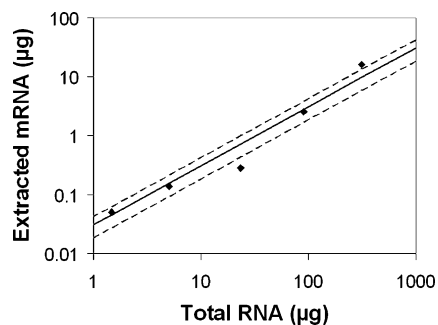


Figure 5. Efficiency of monolithic preconcentrators in extracting mRNA from total RNA shown for five different capillaries with five different loading concentrations of total RNA (diamonds). The average efficiency of the five single replicates (solid line) and standard deviation of the average efficiency (dashed lines) are also represented.

electrophoresis, using an Agilent bioanalyzer to observe the purity of the commercial material. We found significant rRNA (18S and 28S) contamination in the purchased mRNA (Figure 4). After extraction using the PPM, the mRNA appeared to have higher purity (Figure 4). This demonstrates how the mRNA extraction efficiency can be maximal (i.e., at or near 100% of mRNA in the sample) and yet have an extraction efficiency of less than 100% of the commercial poly-A-enriched RNA.

The primary objective of these studies was to demonstrate the ability to trap, concentrate, and purify mRNA. With the monolith optimally functionalized, we then tested the ability of the oligo dT columns to extract and purify mRNA from total RNA (Figure 5). Five different monoliths were tested, which exhibited linear extraction ranging from 1.5 to 5% yield. Even after extracting 16 μg of mRNA from 315 μg of total RNA, the 0.4- μL volume monolith still showed no signs of saturation. With 6 μL of trapping agent, Jiang and Harrison were only able to trap 60 ng.¹² This large improvement in capacity from such a small volume may make it ideal for utilization in microfluidic technologies.

The total amount trapped and the enhanced concentration are important for the end applications. Microarray analysis often requires 0.5–1 μg of purified, highly concentrated, single-stranded genetic material. Microfluidic arrays can add further constraints by reducing the volume of analyte. Thus, in order to meet the demands of arrays in a microfluidic environment, an extraction

Table 1. Comparison of Yields and Integrity of mRNA Extracted in NaCl or TMAC Buffers Using PPM Functionalized with Oligo dT's, 50% LNA Substituted Oligo dT's, and 100% LNA Substituted Oligo dT's to mRNA from Other Commercial Sources ($n = 3$)

type	yield (%)	StDev (%)	260/280	enrichment	StDev
control total RNA	n/a	n/a	2.14	1	n/a
control mRNA	n/a	n/a	2.14	96.2	44.6
poly-A purist mRNA	3.01	0.59	2.16	138.6	70.6
monolith dT mRNA	3.06	1.42	2.18	14.8	6.6
monolith dT-LNA mRNA	3.20	1.23	3.29	45.4	13.6
monolith LNA mRNA	1.86	0.67	2.05	16.2	11.9
monolith TMAC mRNA	2.23	1.06	2.10	109.9	13.0

device must be capable of extracting large quantities of mRNA and eluting it in a small volume. By utilizing PPM, the sample could be sufficiently concentrated and purified to potentially allow direct analysis on a microarray, bypassing postpurification amplification steps and associated biases. In fact, we showed the capacity to extract and elute more than 16 μg of mRNA at concentrations up to 1 $\mu\text{g}/\mu\text{L}$.

The total amount trapped becomes even more important in the context of the size of the monolith. The significance of trapping 16 μg of mRNA on a 0.4- μL (250- μm diameter by 8-mm length) monolith cannot be overstated. Space is of the essence in microfluidic devices. Accordingly, it is essential that any sample preparation technologies included on the device have the capacity of commercial technologies packaged into small spaces. Further, this small monolith size implies scalability. For example, the micro poly-A purist kit, which purifies up to 1 mg of total RNA ($\sim 25 \mu\text{g}$ of mRNA), suspends a dried pellet of oligo dT cellulose ($> 100 \mu\text{L}$ volume) in an even larger amount of solution. Using an identical volume (100 μL) of oligo-dT monolith and assuming linear scalability in trapping, the PPM could trap at least 4 mg of mRNA from 160 mg of total RNA.

The purity of the extracted mRNA was also examined and compared with commercial kits and control mRNA (summarized in Table 1). qPCR was used to determine enrichment of mRNA relative to total RNA. PCR confirmed a 14.8-fold enrichment of monolith purified mRNA over total RNA. In comparison, mRNA purchased from Ambion exhibited an enrichment of 96.2-fold and

mRNA purified using the Ambion poly-A purist kit had an enrichment of 138.6-fold.

While these results confirmed the ability of the monolith functionalized with oligo dT's to trap and purify mRNA from total RNA in NaCl solution, they did not match the results of the best commercial kits. We believe that the failure to purify mRNA from total RNA with greater enrichments was due to nonspecific binding of ribosomal RNA to the monolith and association with the mRNA hybridized to the oligo dT's. However, in order for this miniature mRNA extractor to be truly worthy of microfluidics, it not only must possess the trapping capacity of commercial kits in a microliter scale space but also must meet the demands for quality mRNA purification. This is why we compared the mRNA quantities and qualities of the 0.4- μ L microfluidic, monolith purified mRNA to the highest quality commercial extraction kits (>100- μ L volume of pelleted oligo dT cellulose and nonmicrofluidic extraction with proprietary buffers) and control mRNA. Therefore, we hypothesized that if we could increase the affinity of the oligo dT's for mRNA, that we could increase the stringency of the wash step, thereby improving the overall purity of the extracted mRNA, perhaps matching the yield and purity of the best commercial mRNA with a 0.4- μ L microfluidic PPM. We chose two methods described in the literature: (1) Employ locked nucleic acid substituted oligo dT's.²² (2) Utilize TMAC, which specifically stabilizes the A-T bond.²³

For each of the methods, we performed an optimization of the wash buffer by washing with progressively lower salt concentrations until the bound mRNA eluted. In this fashion, we could perform the most stringent wash possible and gain comparative data. Mixed LNA-dT functionalized PPM showed a 3-fold improvement in enrichment over oligo-dT functionalized PPM. However, 100% LNA substituted dT's did not show any increase in enrichment ($p = 0.8672$), even though the columns were washed in diH₂O. We believe that this is due to the large increases in the affinity of the fully substituted dT's toward anything that binds to them. It is important to note that even if the enrichment was not increased for 100% LNA substituted dT's, the wash step was performed in diH₂O, eliminating salts and other contaminants without having to perform rigorous purification steps as done in other methods.

Utilization of TMAC enabled the wash step temperature to be increased to 90 °C without elution of mRNA. mRNA purified using this method proved to have a statistically equivalent yield to the original monolith purification experiments in NaCl ($p = 0.4627$) in addition to the poly-A purist extracted mRNA ($p = 0.3278$). Further, monolith purified mRNA using TMAC demonstrated equivalent purity to commercial control mRNA ($p = 0.6364$) and mRNA extracted from the poly-A purist kits ($p = 0.5267$). This confirmed our objective of creating a submicroliter size, micro-

fluidic PPM with the equivalent yields, capacity, and purity of commercial kits.

CONCLUSION

We created a photopolymerized monolith in situ, which allows attachment of various probe types in addition to constant flow sample purification, and preconcentration with temperature-controlled binding and elution. We have optimized both trapping and purification of PPMs using oligo dT's, locked nucleic acid substituted dT's, and TMAC solutions and have compared the results with commercially available purification kits and mRNA. Utilization of PPM provided for more efficient trapping, up to 70% efficiency, and larger total yields, at least 16 μ g, than those achieved in other microfluidic devices.¹² Binding and washing in TMAC further improved the enrichment of the mRNA to equal commercial mRNA controls and mRNA extracted from commercial kits. These results demonstrate that both quality and quantity can be achieved in mRNA extraction in PPM, whose size and method of creation make it ideal for microfluidic devices.

While these results are encouraging, it is possible that further refinement of pore size, monolith length or volume, temperatures, and buffers may lead to additional improvements. Increased refinement of the wash step in particular may lead to even greater mRNA purities. We also report for the first time to our knowledge the ability to wash mRNA in pure water, with no additional buffers or salts. Additional research on the use of locked nucleic acids in mRNA purification may lead to simplified procedures that do not require postsample purification to remove salts and buffers. Moreover, the ability to attach probes with primary amines to the PPM may allow it to be used with other technologies, such as peptide nucleic acid substituted oligo dT's, that may also have a significant impact on mRNA purification.²⁴ Already these microfluidic PPM have the potential to bind as much mRNA as commercial kits with statistically equivalent efficiencies and purities. The PPM's small size and high extraction capacity together with its photocastable properties make it an ideal candidate for microfluidic extraction technologies.

ACKNOWLEDGMENT

The authors acknowledge Dr. Timothy Shepodd of Sandia National Laboratories for his invaluable assistance during the performance of this work. B.C.S. performed part of this research while on appointment as a U.S. Department of Homeland Security (DHS) Fellow under the DHS Scholarship and Fellowship Program, a program administered by the Oak Ridge Institute for Science and Education (ORISE) for DHS through an interagency agreement with the U.S. Department of Energy (DOE). ORISE is managed by Oak Ridge Associated Universities under DOE contract DE-AC05-00OR22750. All opinions expressed in this paper are the author's and do not necessarily reflect the policies and views of DHS, DOE, or ORISE.

Received for review May 4, 2007. Accepted May 9, 2007.

AC0709201

(22) Jacobsen, N.; Nielsen, P. S.; Jeffares, D. C.; Eriksen, J.; Ohlsson, H.; Arctander, P.; Kauppinen, S. *Nucleic Acids Res.* **2004**, *32*, e64.

(23) Jacobs, K. A.; Rudersdorf, R.; Neill, S. D.; Dougherty, J. P.; Brown, E. L.; Fritsch, E. F. *Nucleic Acids Res.* **1988**, *16*, 4637-4650.

(24) Phelan, D.; Hondorp, K.; Choob, M.; Efimov, V.; Fernandez, J. *Nucleosides Nucleotides* **2001**, *20*, 1107-1111.